

Modified Tracking Differentiator for Enhancing the Performance of Exoskeleton Knee System Based on Active Disturbance Rejection Control

Nasir Ahmed Alawad¹, Amjad J. Humaidi², Ahmed Sabah Alarejee³

¹Department of Computer Engineering, Faculty of Engineering, Mustansiriyah University, Baghdad, Iraq

²Department of Control and System Engineering, University of Technology, Baghdad, Iraq

³Department of Computer Engineering, University of Technology, Baghdad, Iraq

¹cse.20.33@grad.uotechnology.edu.iq, ²Amjad.j.humaidi@uotechnology.edu.iq,

³ahmed.s.alaraji@uotechnology.edu.iq

Abstract— Exoskeleton robots help users with mechanical forces by recognizing their intentions, and they require a lot of energy efficiency, a lot of load capacity, and a good fit. A basic one degree of freedom (DOF) construction was devised in this work, which was mostly used in the knees of exoskeleton robots. The exoskeleton is a small robotic device used for knee injury training. It is a nonlinear mathematical model with many mechanical factors that might vary and produce uncertainty, as well as external disturbances that can be utilized to monitor control. The transitioning process is frequently organized using tracking differentiator TD to resolve the conflict between system speed and overshoot. An active disturbance rejection control (ADRC) with a modified tracking differentiator is described to tackle these challenges, enhance control accuracy, and reduce settling time for exoskeleton modified trajectory differentiator (MTD). Simulation tests showed that (MTD) reduced the tracking error by 36%, when compared with the improved TD1 and 37.5% for Hans TD2 at uncertainty case. Despite the presence of several model uncertainties, the suggested training knee exoskeleton robot system using the MTD-ADRC was able to achieve the necessary target value. Control design and analysis can be done with Matlab and Simulink

Index Terms— Exoskeleton system, ADRC, MTD, nonlinear calculus, robustness

I. INTRODUCTION

Exoskeleton robots are currently being employed in a variety of industries, including industrial, military, medical, and rehabilitation [1],[2], with associated research being conducted to suit the needs of each field. In recent times, however, robots are being developed in such a way that they may closely support humans in their daily lives or assist them with rehabilitation training [3]. One of the reasons for the change to robot-assisted rehabilitation is a dearth of physiotherapists to instruct these patients. These lower limb robots help patients overcome physical limitations and live normal lives by assisting with muscular strength[4]. They also assist with rehabilitation training so that patients can overcome physical disabilities and lead normal lives. Lokomat (Hocoma, Volketswil, Switzerland), ReWalk Personal (ReWalk Robotics, Marlborough, MA, USA), and HAL (Cyberdyne, Tsukuba, Japan) are three examples of commercialized lower limb exoskeleton robots[5]. In general, there are two categories of rehabilitation devices when the structure of the device is used as the criterion of division. The terminal guidance device is one, while

DOI: <https://doi.org/10.33103/uot.ijccce.23.1.6>

the exoskeleton mechanism is the other [6]. The exoskeleton mechanism for joint rehabilitation is based on the ergonomics principle and consists of a joint rotation axis and a human joint axis.

The exoskeleton system is worn on the human arm, which drives the joint and contacts between the patient's lower limbs and the robot to execute rehabilitative motions. As a result, this procedure is akin to encircling the patient's limb with a structure [7]. The final exoskeleton application is rehabilitation. Exoskeletons for rehabilitation have been created for a variety of uses. They can be used in either the lower or upper limb for gait rehabilitation [8]. The exoskeleton control system can be classed into position, torque/force, and force interaction controllers based on physical factors.

To ensure that the exoskeleton joints revolve in the proper angle, the position control technique is typically used. The PD controller in the ARMin III robot [9] is an example. Low-level controllers are commonly used to implement position controllers. Many control approaches for exoskeleton systems have been developed in the recent decade. In [10], the planned trajectory was hampered by chattering at the output due to the usage of sliding mode control using (PD). To regulate the actuators of the exoskeleton, researchers employed a Linear Quadratic Regulator (LQR) with electromyographical (EMG) activity in [11], which necessitated using the Riccati equation method.

H-infinity control was utilized to create a dynamic output feedback controller for a human swing leg device in [12]. The findings reveal that the proposed controller can stabilize the system and meet a desired time response specification, but it is still ineffective at detecting disturbances. In [13], a nonlinear intelligent controller for the human swing knee joint was proposed employing Adaptive Neural Network control. ADRC is the new paradigm control. In this subject, there is a scarcity of work in exoskeleton design and control. ADRC has been employed for numerous robotic rehabilitation devices for tracking applications in recent years because of its popularity and usefulness.

An ADRC-based method is used to track the human gait trajectory for a lower limb rehabilitation exoskeleton in [14]. The required human gait trajectory is determined from Clinical Gait Analysis, and the experiment results reveal that the suggested ADRC outperforms the standard (PID) controller. In [15], a control approach for improving the tracking performance of the lower limb exoskeleton is given, (ADRC) with fast terminal sliding mode control (FTSMC) can not only alleviate the disturbance but also quickly converge to a confined zone. This article indicates that using a (MTD) improves ADRC and reduces the effect of noise and disturbances here on exoskeleton performance. Designers still need high-order derivatives of the reference signal in the many control techniques. We can achieve this by repeatedly using differentiator. In [16] develop a linear high order tracking differentiator, however it has poor achievements in the field.

The remainder of this work is organized as follows: The Exoskeleton mathematical model is introduced in section .II, design mechanism of the knee joint is examined in section. III dependent on the target trajectory. The design of the ADRC for many TD configurations is achieved in Section IV. MTD has been used to design and analyze the ADRC approach in section V. The trajectory tracking of the knee joint exoskeleton rehabilitation mechanism is realized using different performance indices in section VI. Computer simulation and discussion of closed-loop control approaches is analyzed in section VII. Finally, in section VIII, there are some conclusions.

DOI: <https://doi.org/10.33103/uot.ijccce.23.1.6>

II. EXOSKELETON MATHEMATICAL MODEL

To ensure that the motion is congruent with human knee joint motion without creating secondary injuries, the exoskeleton mechanism for knee joint rehabilitation training should be designed with rehabilitation medicine, mechanical structure principles, and movement mechanisms in mind. The structure of the exoskeleton rehabilitation mechanism for knee joint rehabilitation training is based on the characteristics of the patient's body structure and the feature of knee joint movement [17]. The mechanical and electrical exoskeleton construction is shown in Fig. 1. Using the Lagrange equation, we were able to create a link between the position trajectory and the applied motor torques, resulting in the exoskeleton-human mathematical model [18],[19],[20].

$$J\ddot{\theta} = -\tau_g \cos\theta - f_s \operatorname{sgn}\dot{\theta} - f_v \dot{\theta} + \tau_h + \tau \quad (1)$$

θ is the angle formed by the knee joint between the actual position of the shank and full extension, $\dot{\theta}$ and $\ddot{\theta}$ are the angular velocity and acceleration of the knee joint, respectively.

J , f_s , f_v , τ_g , and τ are the leg inertia, solid friction coefficient, viscous friction coefficient, gravity torque, and the actuating torque, which is applied to the Knee-Exoskeleton system at the knee level, respectively. In this work assuming τ_h as external human disturbance. [18],[19],[20] identifies the human leg-exoskeleton parameters. Table I provides the parameters that the system has identified.

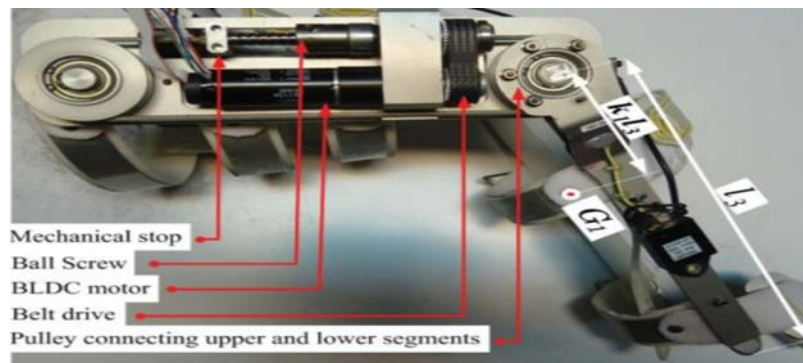


FIG. 1. ORTHOSES AND ITS COMPONENTS.

TABLE I. SYSTEMS IDENTIFIED PARAMETERS

parameter	value
Inertia (J)	0.4 kg.m^2
Solid Friction Coefficient (A)	0.6 N.m
Viscous Friction Coefficient (B)	1 N.m.s./rad
Gravity Torque (τ_g)	5 N.m

III. KNEE JOINT DESIGN MECHANISM

Based on human lower limb structure, a rehabilitation process for the Knee joint exoskeleton is developed. The servo motor is used as the driving force to realize the flexion and extension movement of the knee joint, and the mechanism is engaged with the output shaft gear of the reducer through the arc rack. The motor connects the horizontal connecting rod and the rotating rod through the cross roller bearing to realize the flexion/extension

DOI: <https://doi.org/10.33103/uot.ijccce.23.1.6>

movement of the knee joint. The range of motion of the patient's knee joint is limited by the number of teeth on the driving gear and the arc rack, ensuring the patient's safety.

The results of this study will aid in the restoration of human knee joint motion and the advancement of exoskeleton rehabilitation robot technology. The motion of the rotation center of the human knee joint is achieved by the passive adjustment module, which has a specified activity margin relative to the exoskeleton knee joint, and the rehabilitation mechanism's movement matches the human knee joint's movement. The tracking trajectory for the knee joint exoskeleton rehabilitation mechanism is produced using the closed-loop ADRC iterative learning control method. The desired trajectory is (-0.785rad) at rest position (*Fig.1a*), move to (-1.57rad) for flexion (*Fig.1b*), (-0.785rad) during extension cycle (*Fig.1c*) and (0 rad) for full extension (*Fig.1d*) and repeat this trajectory many times .

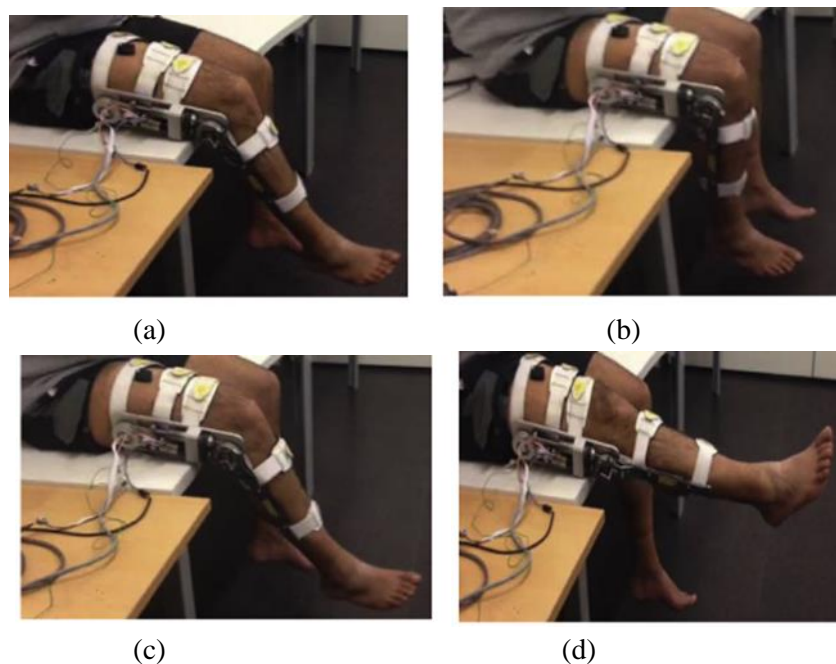


FIG. 2. SHANK POSITIONS DURING FLEXION-EXTENSION: (A) THE REST POSITION,(B) THE SHANK AT FLEXION,(C)THE SHANK DURING EXTENSION POSITION,(D) THE SHANK AT FULL EXTENSION.

IV. ADRC SCHEME

ADRC is a viewpoint control approach that employs a linear extended state observer (LESO) [21],[22],[23],[24], as shown in *Fig. 3*. LESO is a key component of the ADRC design, as it makes use of existing information to interpret states, estimates states online, and eliminates factors such as model parameters, external signals, and uncertainties as a total disturbance. To fulfill transient behavior, feed forward (PD) controllers with linear or nonlinear State Error Feedback (NSEF) are used.

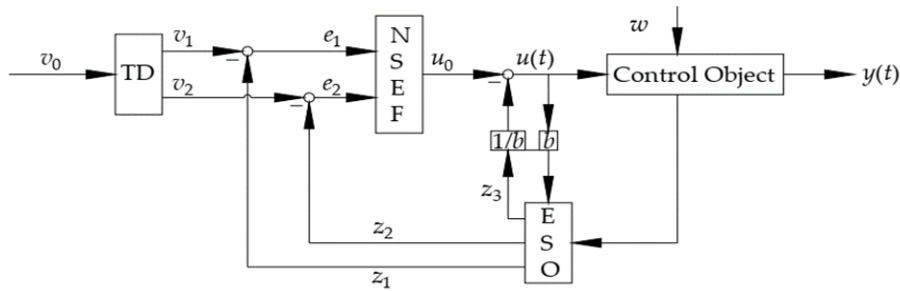


FIG. 3. STRUCTURE OF THE ADRC.

The TD is commonly used to prevent overshoot and improve system response [25]. It works with a transient profile of input signals that has been differentiated to avoid abrupt shifts, resulting in a progressive increase in output rather than abrupt increases. We propose to utilize an MTD instead of Han TD[22] to resolve the contradiction between reaction speed and noise effect in this paper, therefore it can be divided into three parts based on TD:-

A-TDI-ADRC

To eliminate set point jumps in this phase utilizing Han-TD, you must create a transient profile that the plant's output may properly follow. Engineers have designed multiple motion profiles in servo systems, despite the fact that this need is typically neglected in a normal control textbook. This paper provides a basic and easy-to-use solution. For a double integral plant (Han-TD)[22], it is generally known that:

$$\begin{cases} \dot{x}_1 = x_2 \\ \dot{x}_2 = u \end{cases} \tag{2}$$

With $|u| \leq r$ and v_0 is the desired value for x_1 , the time-optimal solution is:-

$$u = -r \operatorname{sign}\left(x_1 - v_0 + \frac{x_2|x_2|}{2r}\right) \tag{3}$$

The following differential equation is solved using this method to produce the desired transient profile:

$$\begin{cases} \dot{v}_1 = v_2 \\ \dot{v}_2 = -r_1 \operatorname{sign}\left(v_1 - v_0 + \frac{v_2|v_2|}{2r_1}\right) \end{cases} \tag{4}$$

The tracking signal of the intended trajectory v is represented by the state variable v_1 , and its derivative is represented by v_2 . Note that the value r_1 can be adjusted to speed up or slow down the transient profile based on the physical constraints in each application, but Han's TD is shown to be the high gain tracking differentiator [26].

B-TD2-ADRC

The improved nonlinear tracking differentiator (INTD) with hyperbolic tangent function [27] is utilized to avoid the noise induced by the sign function in Eq.4. With great precision, the INTD can extract differentiation from any piecewise smooth nonlinear signal. The enhanced tracking differentiator (INTD) has the necessary filtering capabilities and can handle noise-induced nonlinearities.

DOI: <https://doi.org/10.33103/uot.ijccce.23.1.6>

$$\begin{cases} \dot{v}_1 = v_2 \\ \dot{v}_2 = -r_2^2 \tanh\left(\frac{\rho v_1 - (1 - \varepsilon)v_0}{\gamma}\right) - r_2 v_2 \end{cases} \quad (5)$$

The parameters $\rho, \varepsilon, \gamma$ and r_2 are appropriate design parameters, where $0 < \varepsilon < 1, \rho > 0, \gamma > 0$ and $r_2 > 0$. May be change the tanh term by any appropriate nonlinear function that the TD is convergent[28].

C- MTD-ADRC

To increase the tracking differentiator's performance, it's required to remove the tracer's complex solution, particularly the solution on the imaginary axis, and to meet the condition that the tracking differentiator converge rapidly [29],[30]. As illustrated in [31], a better tracking differentiator can be obtained in the following form:-

$$\begin{cases} \dot{v}_1 = v_2 \\ \dot{v}_2 = -1.73\lambda v_2 - \lambda^3(v_1 - v_0) \end{cases} \quad (6)$$

Here, v_1 is the desired trajectory and v_2 is its derivative. The application determines the value of λ , which is chosen to fit the transient profile's space. The "tracking differentiator" of the input signal is then denoted v_2 . Taking λ^3 instead of λ^2 in ref.[31] make the tracking more accuracy.

V. TD-ADRC OPTIMIZATION PARAMETERS

According to Equations (4, 5, 6), there are six unknown tuning parameters ($r_1, r_2, \lambda, \rho, \gamma, \varepsilon$), hence any optimization methods must be used to calculate their values [32],[33],[34]. Ant colony optimization (ACO) is proposed in this paper [35]. The (ACO) is a population-based met heuristic that can be applied to complex optimization problems to obtain approximate solutions. This method is based on an ant's foraging activity when looking for a path between their colony and a source of food. Table II shows the appropriate design parameters for the ADRC algorithm based on TD.

TABLE II. ADRC OPTIMIZATION PARAMETERS WITH DIFFERENT CONFIGURATION

	Parameter	Value
MTD	λ	80.13
TD2	r_2	268.35
	ρ	0.8218
	γ	2.357
	ε	0.1198
TD1	r_1	160.35

In this paper using linear ADRC, where the feed forward PD controller is[36]:-

$$u_o = K_p (v_1 - \hat{z}_1) + K_d (v_2 - \hat{z}_2) \quad (7)$$

\hat{z}_1, \hat{z}_2 are state estimation of y and \dot{y} respectively. The following state space form can be used to express the standard system of Eq. (1) as [22], [37],[38]:

$$\begin{cases} \dot{x}_1 = x_2 \\ \dot{x}_2 = x_3 + b_o \tau \\ \dot{x}_3 = \dot{f} \\ y = x_1 \end{cases} \quad (8)$$

DOI: <https://doi.org/10.33103/uot.ijccce.23.1.6>

where f represents the total disturbance and model uncertainties. The disturbance, represented by x_3 , is estimated by \hat{z}_3 and compensated by the following control law:

$$u = u_o - \hat{z}_3/b_o \quad (9)$$

It is worth noting that the exoskeleton system's actuation torque is equivalent to the control law provided by the above equation. For the system represented by Eq. (1), the proposed structure of observer dynamics is given by:-

$$\begin{aligned} \dot{\hat{z}} &= \mathbf{A} \hat{z} + \mathbf{B} \tau + \boldsymbol{\beta} (y - \hat{y}) \\ \hat{y} &= \mathbf{C} \hat{z} \end{aligned} \quad (10)$$

Where, $\hat{z} = [\hat{z}_1 \ \hat{z}_2 \ \hat{z}_3]^T$ is the vectors of estimates of y , \dot{y} , and f , respectively. The observer described above is known as the Linear ESO and $\boldsymbol{\beta}$ is termed as observer gain matrix. The elements of observer gain matrix $\boldsymbol{\beta}$ can be obtained using the pole-placement method [39]. One can establish the following characteristic equation based on structure of extended state observer

$$Q(s) = |s\mathbf{I} - (\mathbf{A} - \boldsymbol{\beta} \mathbf{C})| = (s + \omega_o)^3 \quad (11)$$

The observe gain matrix can be evaluated as follows:

$$\boldsymbol{\beta} = [3 \omega_o \quad 3 \omega_o^2 \quad \omega_o^3] \quad (12)$$

Only the bandwidth ω_o of the LESO is required to determine the components of the observer gain matrix. This easy tuning strategy, on the other hand, combines the performance and noise-sensitivity trade-offs. The controller bandwidth W_c is used to calculate K_p and K_d for regulator tuning, as follows:

$$\begin{aligned} k_p &= \omega_c^2 \\ k_p &= 2 \omega_c \end{aligned} \quad (13)$$

Where ω_c is related to design specifications, specially the settling time T_s , so that [37]:-

$$\omega_c = \frac{10}{T_s} \quad (14)$$

In this study, if select $T_s=0.4\text{sec}$, then $\omega_c = 24.5\text{rad/sec}$ and the value of observer bandwidth W_o is calculated as [40],[41] :-

$$\omega_o = 4\omega_c$$

Theorem: If the ESO is well-performed, the improved structure of ADRC used for controlling the system described by Eq.(1) can lead to $y \rightarrow v_o$ as $t \rightarrow \infty$.

Proof: If the ESO has been properly designed, and if y_d is firstly and secondly differentiable, then $\hat{z}_1 \rightarrow y$ and $\hat{z}_2 \rightarrow \dot{y}$ as $t \rightarrow \infty$. According to Eq.(7), the value of $u_o \rightarrow \ddot{v}_o \rightarrow \ddot{y}$ as $t \rightarrow \infty$. This leads to $y = v_o$ and satisfied the stability of the proposed method depending on the bounded input bounded output (BIBO) criterion.

VI. PERFORMANCES INDICES

To show the effectiveness of control strategies with different TDs, some performance indices are found in control literature and chosen for comparison are Integral of the absolute magnitude of error (IAE), , Integral square error (ISE),Integral square of the control signal (ISU),Integral absolute of the control signal(IAU)and Root Mean Square Error(R.M.S.E). All these performance indices can be formulated as:

DOI: <https://doi.org/10.33103/uot.ijccce.23.1.6>

$$\begin{aligned}
 IAE &= \int_0^t |(v_o - y)| dt \\
 ISE &= \int_0^t (v_o - y)^2 dt \\
 ISU &= \int_0^t u^2 dt \\
 IAU &= \int_0^t |u| dt \\
 R.M.S.E &= \sqrt{\frac{1}{n} \sum_1^n (v_o - y)^2}
 \end{aligned} \tag{15}$$

Where, v_o is the reference input signal, y is output of the system, and $v_o - y$ denotes the error of the system and u is the control output. IAE, ITAE, ISE, ITSE are known as time-integral criteria which are generic and comprehensive tools to evaluate the performance of a control system, they allow comparing between different controller designs or even different controller structure [42]. In this work, the minimum value of index suggests best performance [43] and the parameters were chosen on that basis. Whereas ISU relates to denote control effort required for a controller and The IAU performance index reflects a measure of chattering reduce in control signal [27]. The simulation results for position tracking of exoskeleton for knee joint, for various TD-ADRC configurations are compared according to these indices.

VII. SIMULATION RESULTS AND DISCUSSION

To study the effect of TD structure on the position tracking of lower knee, two case are analyzed, nominal and uncertainty. The results has been evaluated via numerical simulation using MATLAB programming software. The numerical simulation has used Ode45 as a numerical solver. In addition, the simulation is based on the assumption, the theta angle can operate within the allowable range $0 \leq \theta \leq -90$ degree.

NOMINAL CASE

To evaluate the performance of the LADRC controller, with no payload condition, it works normally (no human torque effect $\tau_h = 0$) and without any disturbances and noises. *Fig. 4* shows performance of the LADRC with three different TD configurations (TD1, TD2, MTD). *Fig. 5* show knee position error between the desired and actual positions. Comparative experiment results show that the MTD-ADRC control method achieves the smallest tracking error which verifies its effectiveness and superiority to TD1-ADRC and TD2-ADRC as listed in Table III. The control efforts shows noisier for TD2-ADRC due to sign function as shown in *Fig.6*.

DOI: <https://doi.org/10.33103/uot.ijccce.23.1.6>

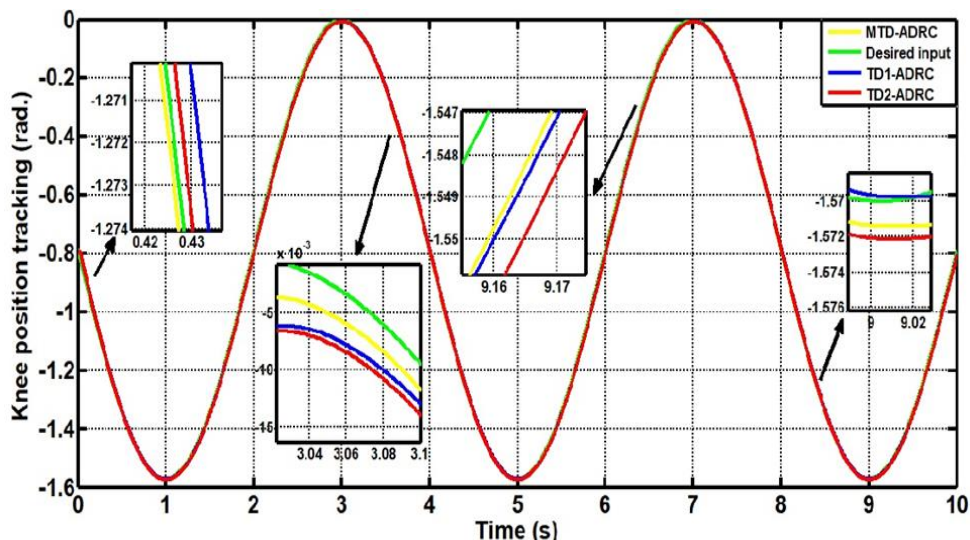


FIG. 4. KNEE POSITION TRAJECTORY FOR COMPARISON BETWEEN DIFFERENT TD CONFIGURATIONS.

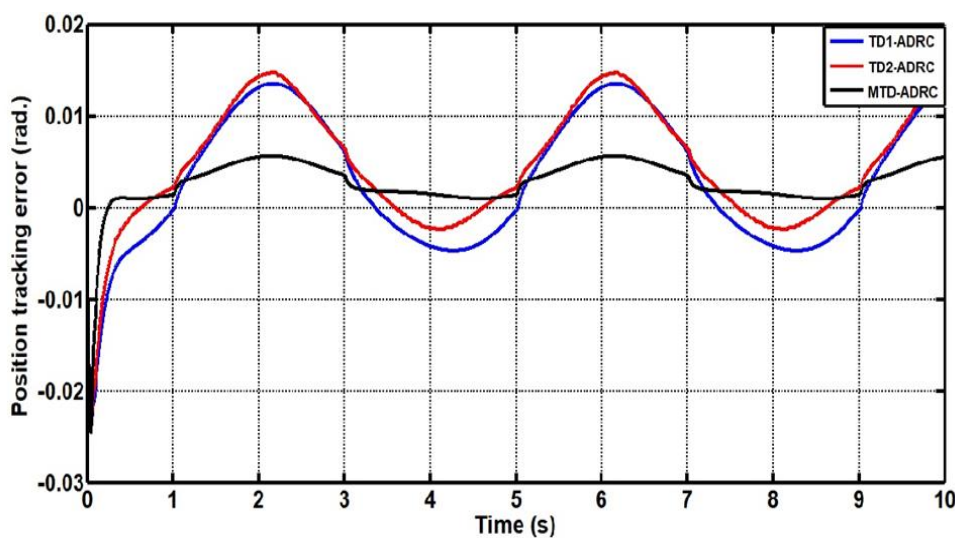


FIG. 5. KNEE POSITION ERROR FOR COMPARISON BETWEEN DIFFERENT TD CONFIGURATIONS.

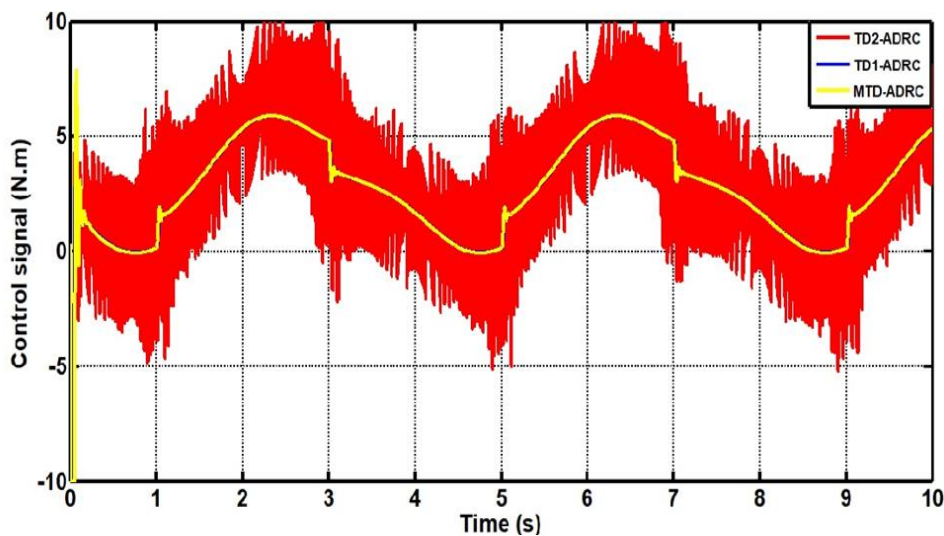


FIG. 6. CONTROL SIGNAL REQUIRED FOR COMPARISON BETWEEN DIFFERENT TD CONFIGURATIONS.

DOI: <https://doi.org/10.33103/uot.ijccce.23.1.6>

TABLE III. PERFORMANCE INDICES FOR DIFFERENT TD-ADRC CONFIGURATIONS

Control Method	IAE(rad.)	ISE(rad.)	ISU(N.m)	IAU(N.m)	R.M.S.E(rad.)
TD1-ADRC	0.064	0.00061	119.2	28.15	0.0078
TD2-ADRC	0.067	0.00063	324	47.6	0.0080
MTD-ADRC	0.031	0.00014	121.2	28.36	0.0038

To see the effectiveness of the ESO, we plot extra state $Z_3(t)$ against its target (total disturbances). Figs. 7, 8, 9 are showed disturbances observation. It is clearly shown that estimate $Z_3(t)$ tracks total disturbances very closely for MTD-ADRC.

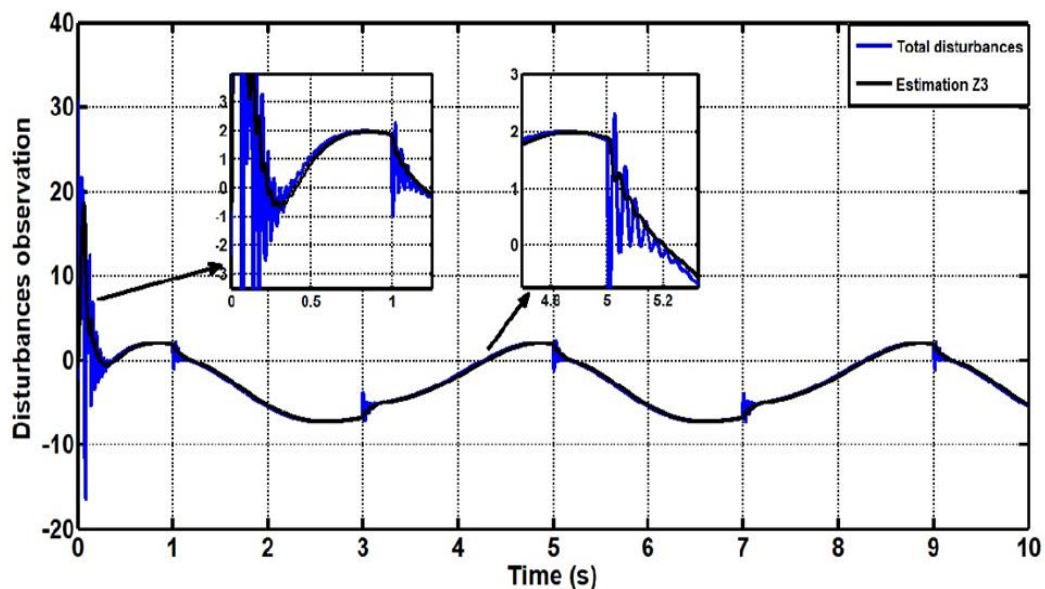


FIG. 7. TOTAL DISTURBANCES AND ITS ESTIMATION FOR TD1-ADRC.

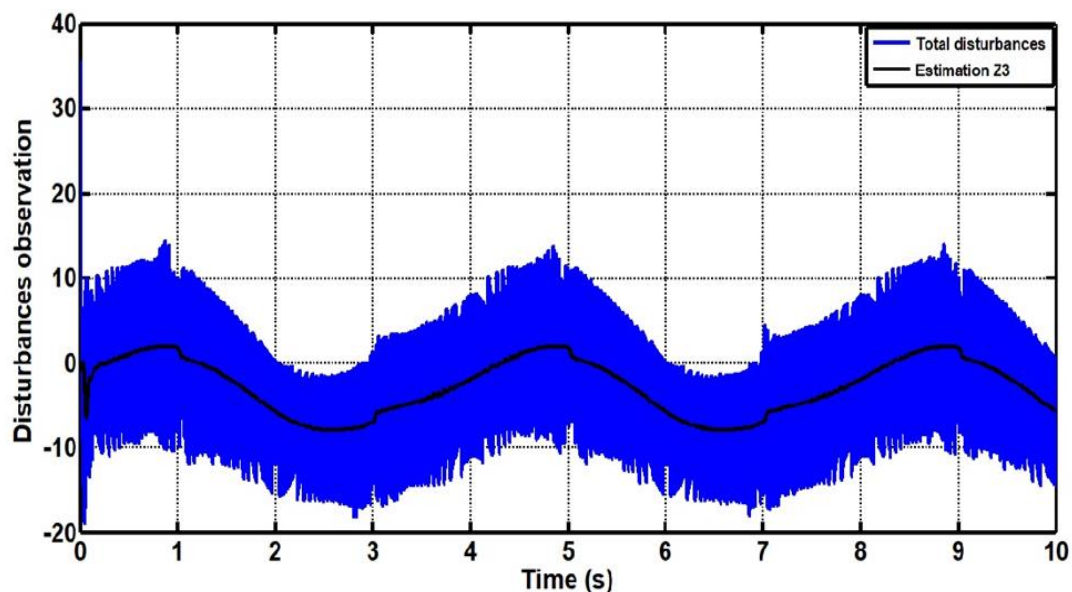


FIG. 8. TOTAL DISTURBANCES AND ITS ESTIMATION FOR TD2-ADRC.

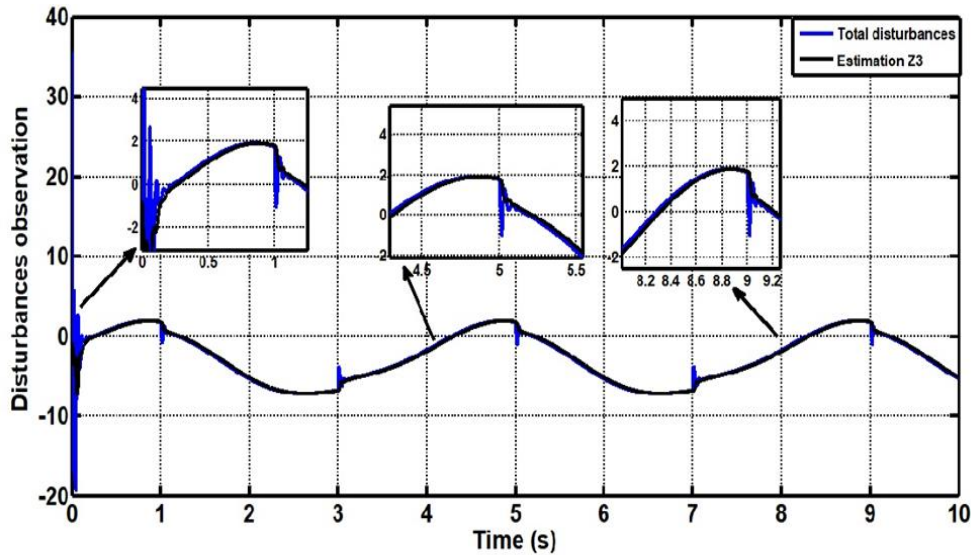
DOI: <https://doi.org/10.33103/uot.ijccce.23.1.6>

FIG. 9. TOTAL DISTURBANCES AND ITS ESTIMATION FOR MTD-ADRC.

UNCERTAINTY CASE

Industrial applications are full of uncertainties. As a result, managing with uncertainties is a constant challenge in controller design. Consider dealing with parametric dynamics uncertainties affected by changes in inertia (J) or frictional factors in the model Eq.(1). Assume in this work, the inertia is increased 100%, so that Table I values are changed to:-

$J = 0.8 \text{ kg.m}^2$, $A = 0.75 \text{ N.m}$, $B = 1.25 \text{ N.m.sec.rad}^{-1}$ and $\tau_g = 6.25 \text{ N.m}$. To evaluate the performance of the LADRC controller, with uncertainty effect. Fig. 10 shows performance of the LADRC with three different TD configurations (TD1, TD2, MTD). Fig. 11 show knee position error between the desired and actual positions. Comparative experiment results show that the MTD-ADRC control method achieves the smallest tracking error which verifies its effectiveness and superiority to TD1-ADRC and TD2-ADRC as listed in Table IV. The control efforts shows more noisy for TD2-ADRC due to sign function as shown in Fig. 12, also the control efforts of both controllers MTD-ADRC and TD1-ADRC are approximately have the same values.

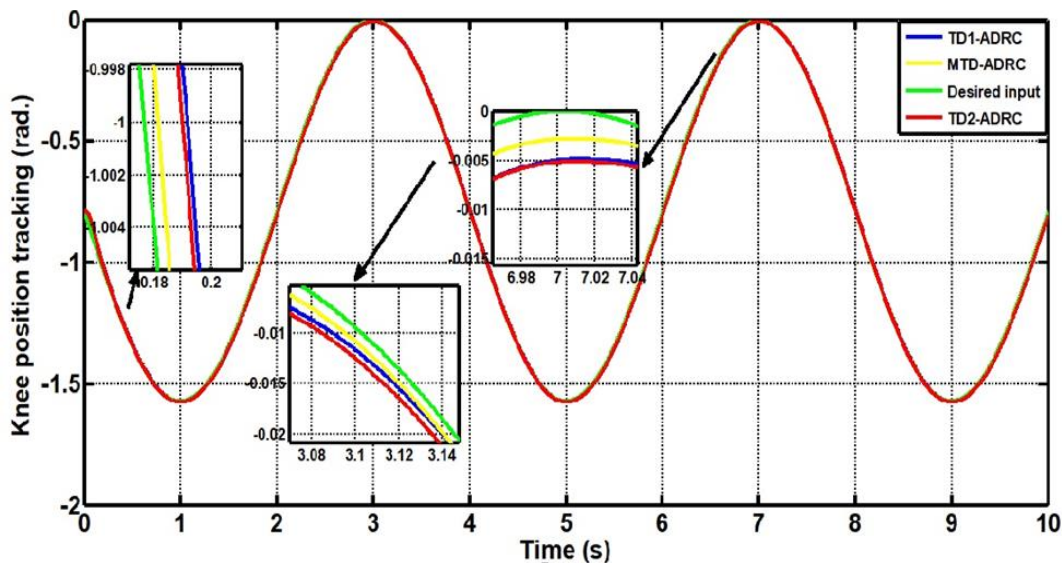


FIG. 10. KNEE POSITION TRAJECTORY FOR COMPARISON BETWEEN DIFFERENT TD CONFIGURATIONS WITH UNCERTAINTY EFFECT.

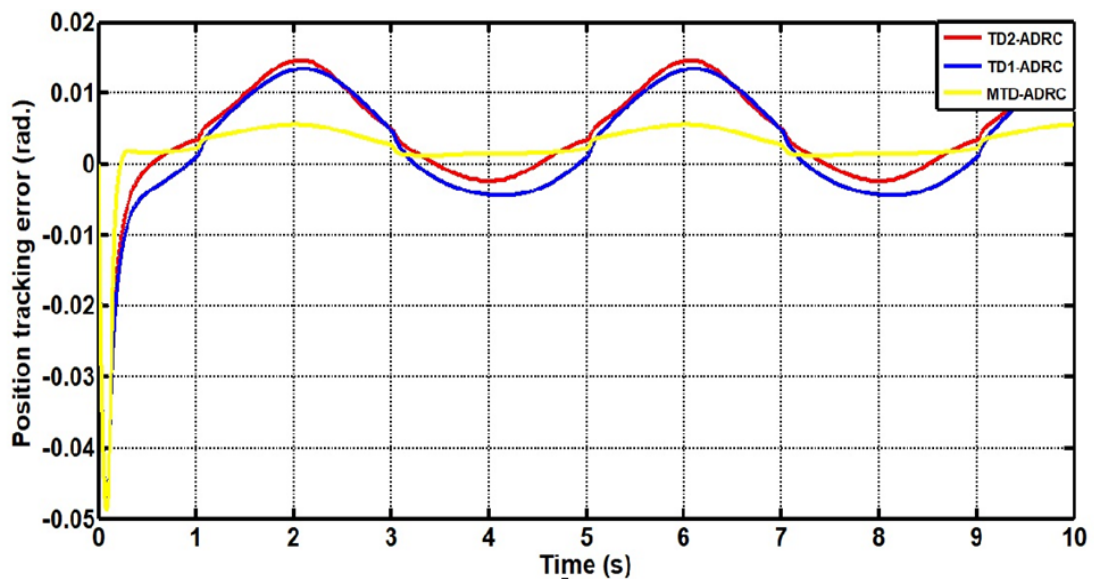
DOI: <https://doi.org/10.33103/uot.ijccce.23.1.6>

FIG. 11. KNEE POSITION ERROR FOR COMPARISON BETWEEN DIFFERENT TD CONFIGURATIONS WITH UNCERTANTY EFFECT.

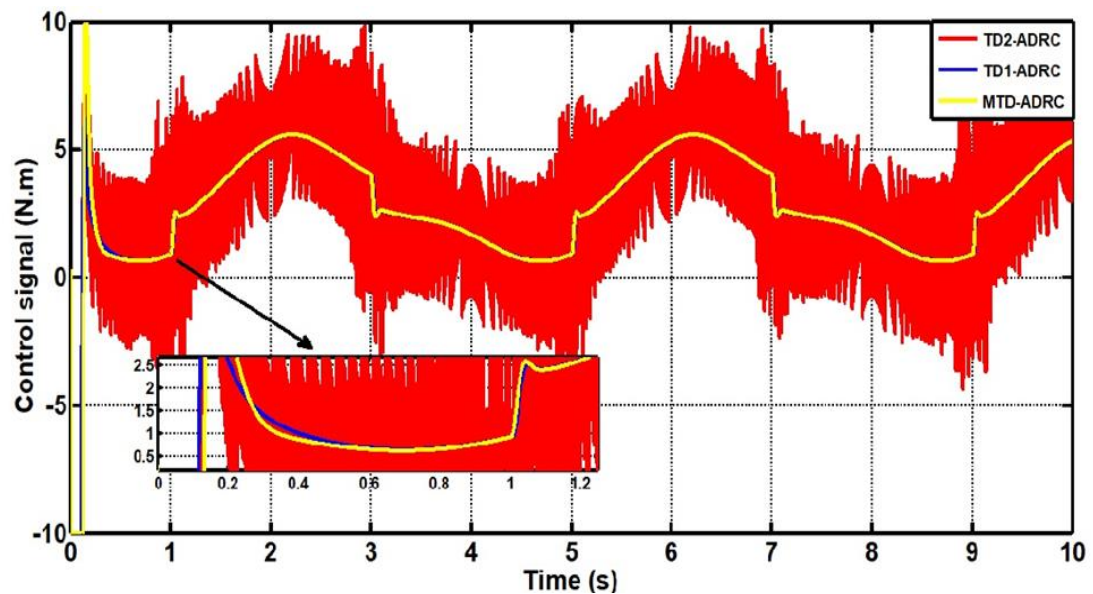


FIG. 12. CONTROL SIGNAL REQUIRED FOR COMPARISON BETWEEN DIFFERENT TD CONFIGURATIONS WITH UNCERTANTY EFFECT.

TABLE IV. PERFORMANCE INDICES FOR DIFFERENT TD-ADRC CONFIGURATIONS WITH UNCERTANTY EFFECT

Control Method	IAE(rad.)	ISE(rad.)	ISU(N.m)	IAU(N.m)	R.M.S.E(rad.)
TD1-ADRC	0.067	0.00079	121.8	29.91	0.0089
TD2-ADRC	0.066	0.00082	325.3	47.72	0.0091
MTD-ADRC	0.036	0.00032	126.6	30.27	0.0057

To see the effectiveness of the ESO, we plot extra state $Z_3(t)$ against its target (total disturbances). Fig.13 is showed disturbances observation. It is clearly shown that estimate $Z_3(t)$ tracks total disturbances very closely for MTD-ADRC.

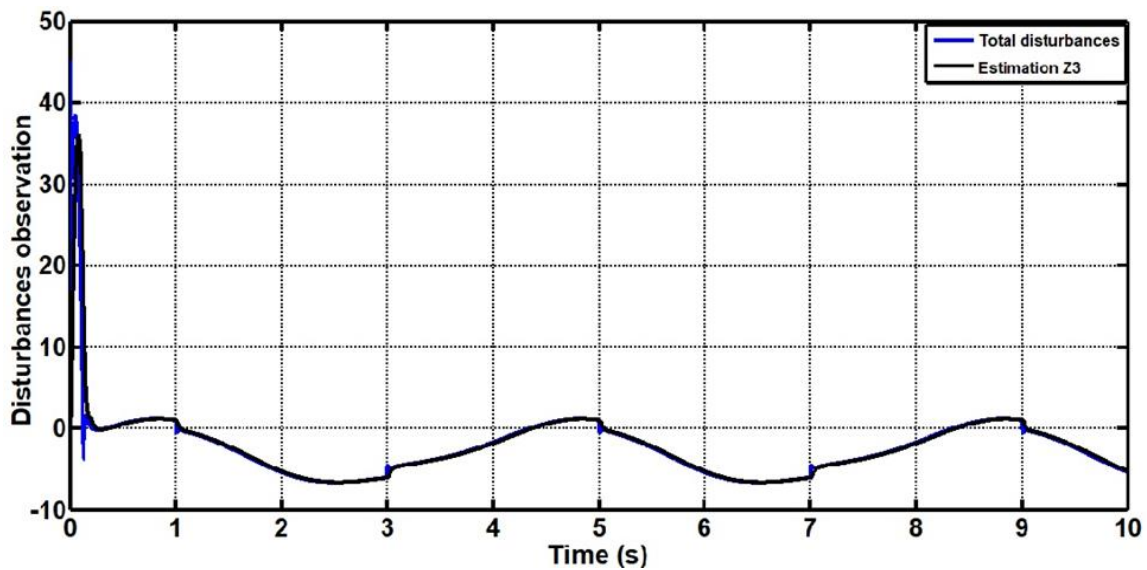
DOI: <https://doi.org/10.33103/uot.ijccce.23.1.6>

FIG. 13. TOTAL DISTURBANCES AND ITS ESTIMATION FOR MTD-ADRC WITH UNCERTAINTY EFFECT.

VIII. CONCLUSIONS

The primary purpose of TD is to smooth the control signal, so that the closed-loop error value between the TD's reference pattern and the predicted by a model states must be very small. In the nominal case, the R.M.S.E for TD1-ADRC, TD2-ADRC, and MTD-ADRC, respectively, are (0.0078, 0.0080, 0.0038). Since there are no inherently nonlinear in the modified TD's construction, such as (sign, tanh), the decrease was very noticeable in the values of the IAE, ISE, and R.M.S.E indices. However, all of these values increased with the uncertainty effect, so the MTD-ADRC is still the best. In general, the simulation findings reveal that the real trajectory is in satisfactory correlation with the desired trajectory, indicating that the knee joint exoskeleton rehabilitation mechanism for MTD-ADRC has improved control and tracking capabilities. Because the values of ISU and IAU are smaller. The control effect signal of the TD1-ADRC is considerably better than that of the TD1-ADRC and MTD-ADRC, according to the simulation results. The transition process must not only take into account the system's numerous restrictions, but it must also adjust to the system's relative order. The proposed framework MTD-ADRC control law is the strongest control aspects that passes from one state to another. The MTD-ADRC results exceed the conventional nonlinear tracking differentiators (TD1 and TD2) in terms of output monitoring, chattering and the response of state variables tracking differentiator estimated is essentially exactly like the real state of the variables of the provided system. The MTD proposed in this study is a stable system in the Lyapunov sense, with global stability and rapid converging. Finally, when tracking, TDM has a basic form and no chattering. It's a superior TD. This study can be extended for future work either by including recent optimization techniques [44],[45], or to design other control schemes to enhancing the ADRC for the purpose of comparison in performance [46],[47],[48].

REFERENCES

- [1] A.A.Blank, J.A.French, A.U.Pehlivan, M.K.O'Malley, "Current trends in robot-assisted upper-limb stroke rehabilitation: Promoting patient engagement in therapy," *Current Physical Medicine and Rehabilitation Reports*, vol.2 ,pp.184–195, 2014.
- [2] M.A.Dzahir, S.I.Yamamoto, "Recent trends in lower-limb robotic rehabilitation orthosis: Control scheme and strategy for pneumatic muscle actuated gait trainers," *Robotics* , vol.3, pp.120–148, 2014.
- [3] W.Pirker, R.Katzenschlager, "Gait disorders in adults and the elderly. Wien. Klin. Wochenschr ,vol.129, pp.81–95, 2017.

Received 27/June/2022; Accepted 01/September/2022

DOI: <https://doi.org/10.33103/uot.ijccce.23.1.6>

- [4] T.Nef, M. Mihelj, G. Kiefer, C. Perndl, R. Muller, R. Riener, "ARMin-Exoskeleton for arm therapy in stroke patients," In Proceedings of the 2007 IEEE 10th International Conference on Rehabilitation Robotics, Noordwijk, The Netherlands, 13–15 June, pp 68–74, 2007.
- [5] M. Visintin, H. Barbeau, N. Korner-Bitensky, N.E. Mayo, "A new approach to retrain gait in stroke patients through body weight support and treadmill stimulation," *Stroke*, vol. 29, pp.1122–1128, 1998.
- [6] Z. Pang, T. Wang, Z. Wang, J. Yu, Z. Sun, and S. Liu, "Design and analysis of a wearable upper limb rehabilitation robot with characteristics of tension mechanism," *Appl. Sci.* vol.10,no.6,pp.1-21,2020.
- [7] S. Christensen and S. Bai, "Kinematic analysis and design of a novel shoulder exoskeleton using a double parallelogram linkage," *J. Mech. Rob.* Vol.10, no.4, pp1-10, 2018.
- [8] K. A. Al-Jumaily, "Active Exoskeleton Control Systems: State of the Art," International Symposium on Robotics and Intelligent Sensors, 2012 (IRIS 2012).
- [9] T.Nef, M. Guidali, R. Riener, "ARMin III—arm therapy exoskeleton with an ergonomic shoulder actuation," *Applied Bionics and Biomechanics*, vol.6, no.2, pp. 127-142,2009.
- [10] A.E.Frisoli, C. Sotgiu, M. Bergamasco, B. Rossi, and C. Chisari, "Design and implementation of a training strategy in chronic stroke with an arm robotic exoskeleton," 2011 IEEE International Conference on Rehabilitation Robotics (ICORR),2011
- [11] G.Aguirre-Ollinger, J.E. Colgate, M.A. Peshkin, A. Goswami, "Active-Impedance Control of a Lower-Limb Assistive Exoskeleton," IEEE 10th International Conference on Rehabilitation Robotics (ICORR), 2007.
- [12] H. I. Ali, "H-infinity Based Full State Feedback Controller Design for Human Swing Leg," *Engineering and Technology Journal*, vol.36, no.3 ,pp.350-357 ,2018.
- [13] Y. Bazargan-Lari, M. Eghtesad, A. R. Khoogar and A. Mohammad-Zadeh, "Adaptive Neural Network Control of a Human Swing Leg as a Double-Pendulum Considering Self-Impact Joint Constraint," *Transactions of the Canadian Society for Mechanical Engineering*, vol.39,no.2, pp. 201-219, 2015.
- [14] Y.Long Y, Z. Du, L. Cong, W. Wang, Z. Zhang, W. Dong , "Active disturbance rejection control based human gait tracking for lower extremity rehabilitation exoskeleton," *ISA Transactions*,vol.67,pp.389-397 ,2017.
- [15] F.Chao,D. Zhijian, H. Long, J. Wang, D. Mei, W. Dong, "Active Disturbance Rejection With Fast Terminal Sliding Mode Control for a Lower Limb Exoskeleton in Swing Phase,"*IEEE Access*,7, pp.72343-72357,2019.
- [16] B. Z. Guo and Z. L. Zhao, "On convergence of tracking differentiator," *Internat. J. Control*, vol.84 ,pp. 693–701, 2011.
- [17] A.Sumit, I. Elamvazuthi, L.Waghmare, B. Patre, F.Meriaudeau, "Improved Active Disturbance Rejection Control for Trajectory Tracking Control of Lower Limb Robotic Rehabilitation Exoskeleton," *Sensors* , vol.20,no.13,pp.1-49, 2020.
- [18] I.Kashif,K.Sherwani, K.Neelesh,C.Ahmed,K.Munna,M.Samer, "RISE-based adaptive control for EICoSI exoskeleton to assist knee joint mobility," *Robotics and Autonomous Systems*, Elsevier, In press, 2019.
- [19] D.Eddine, B.Chouaib ,S.Mefoud, "A robust control scheme based on sliding mode observer to drive a knee-Exoskelton," *Asian Journal of Control*,vol.21,no.10, pp. 439–455, 2019.
- [20] S. Mefoued, "A Second Order Sliding Mode Control and a Neural Network to Drive a Knee Joint Actuated Orthosis," *eurocomputing*,vol.155, pp.1-23, 2014.
- [21] Z.Gao, Y. Huang, J. Han, "An alternative paradigm for control system design," In Proceedings of the 40th IEEE Conference on Decision and Control, Orlando,4–7, vol.5, pp. 4578–4585,2001
- [22] J. Q. Han, "From PID to active disturbance rejection control," *IEEE Transactions on Industrial Electronics*,vol.56,no.3, pp. 900–906, 2009.
- [23] A. J. Humaidi, M.Hussein , A. Ahmed , "Design of Active Disturbance Rejection Control for Single-Link Flexible Joint Robot Manipulator," 22nd International Conference on System Theory, Control and Computing, 2018.
- [24] W.H.Chen, J.Guo, L.Li, "Disturbance-observer-based control and related methods: An overview,"*IEEE Trans. Ind. Electron* ,vol.63,pp. 1083–1095, 2015.
- [25] L.Zhao, X.Liu, T.Wang, B. Liu, "A reduced-order extended state observer-based trajectory tracking control for one-degree-of-freedom pneumatic manipulator," *Adv. Mech. Eng*,vol.10,no.4,pp.1-9, 2018.
- [26] B. Z. Guo and Z. L. Zhao, "Weak convergence of nonlinear high-gain tracking differentiator," *IEEE Trans. Automat. Control*, vol.58 ,pp.1074–1080, 2013.
- [27] I.K. Ibraheem, W.R. Abdul-Adheem, "On the Improved Nonlinear Tracking Differentiator based Nonlinear PID Controller Design," *International Journal of Advanced Computer Science and Applications*, vol.7,no.10, pp.234-241, 2016.
- [28] B.Z.Guo,Z.L. Zhao, "Active disturbance rejection control: Theoretical perspectives," *Communications in Information and Systems* ,vol.15,no.3,pp.361–421, 2015.
- [29] G.H,Qiao, M.L.Sun, R. Zhang, "An Improved Self-Adaptive Tracking Differentiator," *International Conference on Information and Automation,ICIA '09*,pp.152-156, 2009.
- [30] J.H.Wang,J.L.Zhang, J. Yan, "A New Second Order Nonlinear Tracking Differentiator and Application," 2010 International Conference on Computer Design and Applications (ICCD), V1-318-V1-322, 2010.

DOI: <https://doi.org/10.33103/uot.ijccce.23.1.6>

- [31] Y.Ruitao,W.Ping, "Active Disturbance Rejection Control for Single-Phase PWM Rectifier," J Electr Eng Technol, vol.13,no.6,pp. 2354-2363, 2018.
- [32] T. Luay, "Optimal tuning of linear quadratic regulator controller using ant colony optimization algorithm for position control of a permanent magnet dc motor," Iraqi Journal of Computers, Communication, Control and System Engineering,vol.20,no.3,pp. 29-41,2020.
- [33] F. Hassan, L. Rashad, "Particle swarm optimization for adapting fuzzy logic controller of SPWM inverter fed 3-phase IM," Engineering and Technology Journal, vol.29, no.14, 2912-2925, 2011.
- [34] L. Jasim, M. Jasim, "Investigating the Guidance Feature of Searching in the Genetic Algorithm," Iraqi Journal of Computers, Communication, Control and System Engineering, Vol.14, No.1, 2014.
- [35] A. Colomi, M. Dorigo, and V. Maniezzo, "Distributed optimization by ant colonies," Proceedings of ECAL'91, European Conference on Artificial Life, Elsevier Publishing, Amsterdam, 1991.
- [36] N.A.Alawad , A. J. Humaidi., A.S. Al-Araji , "Improved Active Disturbance Rejection Control for the Knee Joint Motion Model," Mathematical Modelling of Engineering Problems,vol.9,no.2,pp.477-483, 2022.
- [37] A.Humaidi, H. Badr, A. Hameed, "PSO-based Active Disturbance Rejection Control for Position Control of Magnetic Levitation System,"5th International Conference on Control, Decision and Information Technologies, pp. 922-928,2018.
- [38] A.Aljuboury, A. Hameed, A. Ajel, A.Humaidi, A.Alkhayyat, A.Mhdawi, "Robust Adaptive Control of Knee Exoskeleton-Assistant System Based on Nonlinear Disturbance Observer," Actuators, vol.11,pp.1-18, 2022.
- [39] Z.Gao, "Scaling and bandwidth-parameterization based controller tuning,"American Control Conference, vol.6, pp. 4989-4996, 2003.
- [40] X.Chen, D.Li,Z. Gao,C.Wang, "Tuning Method for Second-order Active Disturbance Rejection Control," Proceedings of the 30th Chinese Control Conference,pp.6322-6327, 2011.
- [41] N. A. Alawad, A. J. Humaidi, A. Sh. Mahdi Al-Obaidi, A.S. Alaraj, "Active Disturbance Rejection Control of Wearable LowerLimb System Based on Reduced ESO," Indonesian Journal of Science & Technology ,vol.7,no.2,pp. 203-218,2022.
- [42] M.S.Tavazoei, "Notes on integral performance indices in fractional-order control systems," J. Process. Control, vol.20, pp.285-291, 2010.
- [43] R.C.Dorf, R.H. Bishop, "Modern Control Systems," Pearson: London, UK, 2011.
- [44] S. Saadoon , A. Karim , S. Turne, "Optimizing Artificial Neural Networks Using Levy-Chaotic Mapping on Wolf Pack Optimization Algorithm for Detect Driving Sleepiness," Iraqi Journal of Computers, Communication, Control and System Engineering, Vol.22, No.3,pp.128-136,2022.
- [45] I. Ibrahim, H. Ali, "Quantitative PID Controller Design using Black Hole Optimization for Ball and Beam System," Iraqi Journal of Computers, Communication, Control and System Engineering, Vol.21, No.3,pp.65-75,2021.
- [46] N. A. Alawad, A. J. Humaidi, and A. S. Al-Araji, "Observer Sliding Mode Control Design for lower Exoskeleton system:Rehabilitation Case,"Journal of Robotics and Control, vol. 9, no. 2, pp. 477-483, 2022.
- [47] N. A. Alawad, A. J. Humaidi, and A. S. Al-Araji, "Fractional proportional derivative-based active disturbance rejection control of knee exoskeleton device for rehabilitation care," Indonesian Journal of Electrical Engineering and Computer Science, vol.28, no. 3, pp. 1405-1413, 2022.
- [48] N. Ahmed, A. Humaidi, A. Sabah, "Clinical trajectory control for lower knee rehabilitation using ADRC method," Journal of Applied Research and Technology, vol. 20, no.5,pp.576-583, 2022.